J. Electrochem. Sci. Eng. **16** (2026) 3486; https://doi.org/10.5599/jese.3486

Open Access : : ISSN 1847-9286
https://pub.iapchem.org/ojs/index.php/JESE

Original scientific paper

Corrosion inhibition of carbon steel in acidic media by *Annona muricata* leaf extract: electrochemical, adsorption and spectroscopic insights

Karin Paucar[1], Gabriel A. Carrijo-Gonçalves[2], Jesus M. Falcón[3] and Abel Vergara[1,✉]

[1]*Reseach Group in Corrosion and Materials (GI CORRMAT), Chemical Engineering and Textile Faculty, Universidad Nacional de Ingeniería, Av. Tupac Amaru, No. 210, Rimac, Lima, Perú*
[2]*Chemical Engineering Department, Polytechnique School, University of São Paulo, Av. Lineu Prestes, No. 580, São Paulo, São Paulo, Brazil*
[3]*Environmental Engineering Department, San Ignacio de Loyola University, Av. La Fontana, No. 550, La Molina, Lima, Perú*

Corresponding Author: ✉mailto:*avergara@uni.edu.pe*; Tel.: +51-1-932103284; Fax: +51-1-932103284

Received: June 6, 2026; Accepted: August 13, 2026; Published: August 19, 2026

Abstract

Despite the increasing interest in plant-derived green corrosion inhibitors, the inhibition mechanism of Annona muricata leaf extract for carbon steel in acidic media remains largely unexplored. In this study, the corrosion inhibition performance of an ethanolic extract of Annona muricata leaves was systematically investigated for SAE 1008 carbon steel in 1 mol L^{-1} HCl, combining gravimetric measurements and electrochemical techniques, electrochemical impedance spectroscopy and potentiodynamic polarization curves. Complementary, Raman spectroscopy and scanning electron microscopy were used for surface characterization. Phytochemical screening confirmed the presence of several bioactive metabolites such as alkaloids, tannins, phenolic compounds, flavonoids, and lactones, which may contribute to the adsorption capability of the extract. The extract exhibited concentration-dependent inhibition, reaching approximately 92 % efficiency at 6 vol.%. Adsorption analysis showed that the inhibition process follows the Langmuir isotherm, suggesting the formation of a protective organic monolayer on the steel surface. Electrochemical measurements showed a decrease in corrosion current density and an increase in charge transfer resistance in the presence of the inhibitor. Potentiodynamic polarization results revealed that the extract acts as a mixed-type inhibitor. Surface analyses confirmed the adsorption of organic species and the formation of a protective film that reduces corrosion damage. These findings provide new mechanistic insights into the corrosion inhibition behaviour of Annona muricata leaf extract and

demonstrate its potential as a sustainable, environmentally friendly corrosion inhibitor for carbon steel in acidic environments.

Keywords
Green corrosion inhibitor; surface analysis; phytochemical screening; corrosion resistance; weight loss; electrochemical analysis; adsorption isotherms

Introduction

Carbon steels such as SAE 1008 are widely used in industrial applications due to their low cost and favourable mechanical properties. Therefore, this material is commonly employed in pipelines, storage tanks, structural components, and equipment frequently exposed to acidic environments during processes such as pickling, descaling, and acid cleaning [1]. However, these materials are highly susceptible to corrosion in acidic and saline environments [2-4]. Acidic corrosion processes result in significant economic losses and safety concerns, motivating the continuous development of efficient and environmentally benign corrosion protection strategies [5].

Among available corrosion control methods, corrosion inhibitors are among the most practical and cost-effective approaches [2,4]. Inhibitors act by adsorbing onto the metal surface and forming a protective film that reduces anodic metal dissolution and/or cathodic hydrogen evolution reactions [6-9]. Traditional inhibitors, such as chromates and synthetic organic compounds, are highly effective but pose serious environmental and health risks because of their toxicity and persistence [10].

Consequently, there is a growing demand for sustainable and biodegradable corrosion inhibitors derived from natural sources [6,11,12]. Plant extracts have gained considerable attention as green inhibitors because they are renewable, biodegradable, and rich in organic molecules containing heteroatoms (O, N, S and P) and π-electron systems capable of interacting with metallic surfaces [3-5,11]. Nevertheless, their practical implementation is hindered by the lack of mechanistic understanding and standardized evaluation protocols.

Numerous studies have reported high inhibition efficiencies for plant extracts in acidic environments [9,12-15], often attributed to adsorption mechanisms described by Langmuir, Temkin, Freundlich, or El-Awady isotherms. Electrochemical investigations have shown that most plant-based inhibitors behave as mixed-type inhibitors [1,16], while surface characterization techniques such as scanning electron microscopy (SEM), Raman spectroscopy, X-ray photoelectron spectroscopy (XPS), and atomic force microscopy (AFM) have confirmed the formation of protective films on metal surfaces [14,15,17].

Despite the rapid growth of research on green corrosion inhibitors, several challenges remain. Many studies are empirical, with limited insight into adsorption mechanisms, structure-activity relationships, and how extraction conditions affect inhibitory performance. Moreover, the correlation between phytochemical composition and electrochemical behaviour is still poorly understood, highlighting the need for systematic and mechanistic investigations.

Annona muricata L. (soursop) is a tropical plant widely distributed in South America and other tropical regions and is traditionally used for nutritional and medicinal purposes [18]. In Peru, soursop is cultivated in regions between 0 m and 600 m above sea level, mainly in La Libertad, Loreto, San Martín, Ucayali, Ica, and Lima [19]. Its pulp, peel, leaves, fruits, and seeds contain a wide variety of bioactive compounds, including alkaloids, acetogenins, flavonoids, tannins and phenolic compounds, which exhibit antioxidant and antimicrobial properties [20].

Although *Annona muricata* has been extensively investigated for its pharmacological, antimicrobial, and antioxidant properties, its potential as a green corrosion inhibitor remains largely unexplored. These phytochemicals possess heteroatoms and aromatic structures that can promote strong adsorption onto metal surfaces, suggesting that *A. muricata* extracts may act as efficient green corrosion inhibitors [21].

Moreover, comprehensive studies combining gravimetric analysis, electrochemical techniques, adsorption modelling, Raman spectroscopy, and surface morphology to elucidate the inhibition mechanism of *A. muricata* leaf extract for SAE 1008 carbon steel in hydrochloric acid solution have not been previously reported. This integrated mechanistic approach is the main novelty of the present work and contributes to a deeper understanding of the relationship between phytochemical composition, adsorption behaviour, and corrosion protection.

Therefore, the ethanolic extract of *Annona muricata* leaves was investigated as a green corrosion inhibitor for SAE 1008 carbon steel in 1.0 mol L^{-1} HCl solution in this work. The inhibition performance was evaluated using gravimetric measurements, electrochemical impedance spectroscopy, linear polarization resistance, and potentiodynamic polarization curves (Tafel slopes). Adsorption isotherm models were applied to provide insights into the interaction mechanism between the phytochemical constituents of the extract and the metal surface, employing the weight loss results from gravimetric measurements. Surface characterization was performed using scanning electron microscopy (SEM) and Raman spectroscopy to elucidate the adsorption behaviour and protective film formation.

Experimental

Materials and sample preparation

SAE 1008 carbon steel was used as the substrate material. This material is widely employed in industrial equipment, storage tanks, pipelines, and structural components. The chemical composition was: 0.10 wt.% C, 0.03 wt.% Si, 0.50 wt.% Mn, 0.025 wt.% P, 0.025 wt.% S, 0.02 wt.% Al, 0.0008 wt.% B, and Fe balance. Rectangular samples with dimensions of 2.5×5.0×0.02 cm were prepared for electrochemical experiments. Prior to testing, the samples were mechanically abraded using silicon carbide (SiC) abrasive papers (sandpaper) with grit sizes of 80, 220, 400, 600 and 1000. The samples were then ultrasonically cleaned in ethanol and air dried.

Gravimetric and electrochemical tests were performed by immersing the steel samples in 1.0 mol L^{-1} HCl solution (one of the most widely used acids in industrial pickling, descaling and acid cleaning) in the absence and presence of the ethanolic extract of *Annona muricata L.* at concentrations of 1, 2, 4, 6 and 8 col-%. All tests were conducted in triplicate to ensure reproducibility.

Extraction process and phytochemical analysis

Leaves of *Annona muricata* were collected at the “FORTU” Nursery (km 23, Panamericana Sur, Lima, Peru). The collected leaves were dried at room temperature under natural air circulation. The dried leaves were ground and sieved (Tyler system) to pass through a 10-mesh sieve and stored in a desiccator in paper bags until extraction.

The ethanolic extract was prepared by magnetic stirring of the powdered leaves in ethanol for 2 h. After extraction, the mixture was vacuum filtered, and the filtrate was used as the stock solution for inhibitor preparation. Preparation of ethanolic extract of *Annona muricata* leaf is schematically presented in Figure 1. Phytochemical analysis of the extract was carried out following the procedure described in previous work by Coria-Téllez *et al.* [22] and Moghadamtousi *et al.* [23], allowing qualitative identification of major phytochemical groups such as alkaloids, phenolics, flavonoids, and tannins.

Figure 1. *Schematic representation of the preparation of Annona muricata leaves and the subsequent ethanolic extraction procedure used to obtain the crude plant extract employed as a green corrosion inhibitor*

Gravimetric tests

For mass loss experiments, steel samples with dimensions of 4.0×1.0×0.2 cm were used. Prior to immersion, the samples were mechanically abraded using silicon carbide (SiC) abrasive papers (sandpaper) with grit sizes of 80, 220, 400, 600 and 1000. The samples were then ultrasonically cleaned in ethanol and air-dried.

The immersion tests were conducted in accordance with ASTM G31, which provides the standard practice for laboratory immersion corrosion testing of metals. The samples were immersed in 50 mL of 1.0 mol L^{-1} HCl solution, with and without different concentrations of ethanolic extract of Annona muricata L. (1, 2, 4, 6 and 8 vol.%), for 2 h at room temperature. After the immersion period, the samples were removed from the test solution and cleaned in accordance with the recommendations of ASTM G31 to remove corrosion products without affecting the base metal. Subsequently, the samples were rinsed with distilled water, washed with ethanol, dried under a hot air stream, allowed to reach room temperature in a desiccator, and finally weighed using an analytical balance (Sartorius TE214S, precision 0.1 mg).

The inhibition efficiency (η / %) was calculated from weight loss measurements using Equation (1) [1,15], where C_{R0} and C_{Ri} represent the corrosion rates of carbon steel in the absence and presence of the inhibitor, respectively.

$$\eta = \left(1 - \frac{C_{Ri}}{C_{R0}}\right) 100 \quad (1)$$

The corrosion rate (C_R) was determined from the mass loss data using Equation (2) [1], where ΔW / g is the average weight loss, A / cm^2 is the total exposed surface area and t / day is the immersion time.

$$C_R = \frac{\Delta W}{At} \quad (2)$$

From the inhibition efficiency values, the surface coverage degree (θ) was calculated by dividing η by 100 and used to evaluate the adsorption behaviour of the inhibitor on the steel surface. The adsorption data were fitted to different adsorption isotherm models, including Langmuir,

Freundlich, Temkin, Flory-Huggins, and Frumkin isotherms, using linear regression analysis of the experimental data.

Electrochemical measurements

Electrochemical measurements were carried out using a conventional three-electrode cell connected to a Gamry Reference 600 potentiostat/galvanostat controlled by Gamry Framework software. The carbon steel sample served as the working electrode with an exposed surface area of 0.7238 cm^2, employing 1.0 mol L^{-1} HCl solution as electrolyte. A platinum foil and a saturated calomel electrode (SCE) were used as the counter and reference electrodes, respectively.

The open circuit potential (OCP) was measured for 1 h to guarantee a stable potential for the electrochemical tests. Electrochemical impedance spectroscopy (EIS) measurements were conducted over a frequency range of 100 kHz to 100 mHz, at 10 mV (OCP). The EIS were quantitatively analysed using ZView software [1] by fitting the experimental data to appropriate equivalent electrical circuit models. Finally, potentiodynamic polarization (Tafel slopes) curves were recorded from -200 to +200 mV around OCP at a scan rate of 0.5 mV s^{-1}.

Surface characterization

The surface morphology of the steel samples after immersion in 1.0 mol L^{-1} HCl solution for 2 h in the absence and presence of the inhibitor was examined using a Quanta 250 scanning electron microscope (SEM). After immersion, the samples were rinsed with distilled water, ethanol, dried with hot air and stored in a desiccator prior to analysis.

Raman spectroscopy

Raman spectra were recorded from (i) the carbon steel surface immersed in 1.0 mol L^{-1} HCl solution without inhibitor, (ii) the solid inhibitor obtained by evaporating the ethanol solvent, and (iii) the inhibitor film formed on the steel surface after 2 h of immersion in the inhibited acidic solution. Raman measurements were performed using a Horiba Xplora Raman spectrometer equipped with a microscope.

Results and discussion

Phytochemical composition and corrosion inhibition potential

It is important to emphasize that the objective of the present work was not to isolate or identify the individual phytochemical constituents responsible for the inhibition process, but rather to evaluate the corrosion inhibition potential of the crude ethanolic extract of *Annona muricata* leaves obtained through a simple and low-cost extraction procedure. Therefore, the qualitative phytochemical screening was intended to provide an overview of the major classes of secondary metabolites present in the extract.

The phytochemical screening of the ethanolic extract of *Annona muricata* leaves revealed a complex composition rich in organic metabolites with potential adsorption capability. Qualitative tests indicated the presence of alkaloids (Table 1), confirmed by positive responses in Mayer, Wagner and Popoff reactions (+), and more pronounced responses in Dragendorff, Bouchardat, and Sonnenschein assays (++), evidencing a moderate to significant concentration of nitrogen-containing compounds in the extract. The variability in response intensity suggests the coexistence of different alkaloid subclasses with distinct structural features and reactivities.

Table 1. *Phytochemical screening of the ethanolic extract of Annona muricata leaves*

Test		Results
Alkaloids	Mayer reaction	+
	Dragendorff reaction	++
	Bouchardat reaction	++
	Wagner reaction	+
	Sonneschein reaction	++
	Popoff reaction	+
Tannins		++
Phenols		++
Saponins		-
Lactones		++
Flavonoids		++

Legend: (-) no metabolite observed; (+) low evidence; (++) evidence; and (+++) high evidence

In addition to alkaloids, tannins, phenols, lactones, and flavonoids were clearly detected with moderate evidence (++), while saponins were not observed under the experimental conditions used. The consistent detection of phenolic compounds and flavonoids is particularly relevant, as these classes are characterized by aromatic rings bearing hydroxyl groups that can donate electron density [24,25]. Tannins, known for their polyphenolic structure, further contribute to the high density of oxygenated functional groups within the extract [25]. Lactones, although less discussed in corrosion studies, may also participate in adsorption through carbonyl functionalities [26].

The predominance of phenolic and flavonoid constituents suggests that the inhibition mechanism is strongly governed by adsorption processes driven by π-electron interactions and lone-pair donation from oxygen atoms [24]. Alkaloids, containing nitrogen heteroatoms, may enhance adsorption through donor-acceptor interactions with vacant d-orbitals of iron atoms on the steel surface [26]. In an acidic medium, protonation of these species may also promote electrostatic interactions with negatively charged sites formed on the metal interface [24,25].

The absence of saponins indicates that the inhibitory performance is unlikely to be associated with surfactant-type micelle formation or precipitation phenomena. Instead, the chemical profile supports a mechanism dominated by interfacial adsorption and formation of a compact organic film [27,28].

Although a detailed economic assessment was beyond the scope of the present work, the proposed inhibitor offers inherent cost-effectiveness because it is obtained from readily available plant biomass using a simple ethanol extraction process, without requiring complex synthesis, purification steps, or expensive precursors.

Gravimetric analysis

The gravimetric results clearly demonstrate the corrosion inhibitory effect of the leaf extract on SAE 1008 carbon steel. The corrosion rate of the negative control (absence of corrosion inhibitor) in 1 mol L^{-1} HCl (Table 2) was (0.0189 ± 0.0011) g cm^{-2} day^{-1}. The addition of the *Annona muricata* leaf extract caused a pronounced reduction in corrosion rate, decreasing to (0.0051 ± 0.0007) g cm^{-2} day^{-1} at 1 vol.%, corresponding to an inhibition efficiency of (73.02 ± 0.25) % and a surface coverage (θ) of (0.7302 ± 0.0025). Increasing the concentration to 2 % further reduced the corrosion rate to (0.0023 ± 0.004) g cm^{-2} day^{-1}, raising the efficiency to (87.83 ± 0.71) %.

Maximum performance was observed between 4 and 6 vol.%, where corrosion rates reached 0.0018 ± 0.0006 and 0.0015 ± 0.0005 g cm^{-2} day^{-1}, corresponding to efficiencies higher than 90 %. At 8 vol.%, however, a slight decrease in performance was observed (C_R = 0.0021 ± 0.0004 g cm^{-2} day^{-1}; η = 88.89 ± 0.74 %), suggesting that beyond the optimal concentration range, possible intermolecular interactions or partial aggregation in solution may limit additional surface adsorption.

Table 2. *Corrosion rate, inhibitory efficiency and coverage degree at different concentrations of* Amonna muricata *leaf extract at 21 °C*

Concentration, vol.%	C_R / g cm^{-2} day^{-1}	η / %	θ
Negative control	(0.0189 ± 0.0011)	-	-
1	(0.0051 ± 0.0007)	(73.02 ± 0.25)	(0.7302 ± 0.0025)
2	(0.0023 ± 0.0004)	(87.83 ± 0.71)	(0.8783 ± 0.0071)
4	(0.0018 ± 0.0006)	(90.48 ± 0.37)	(0.9048 ± 0.0037
6	(0.0015 ± 0.0005)	(92.06 ± 0.65)	(0.9206 ± 0.0065)
8	(0.0021 ± 0.0004)	(88.89 ± 0.74)	(0.8889 ± 0.0074)

The observed concentration-dependent decrease in corrosion rate indicates that the inhibition process is governed by adsorption phenomena. The progressive increase in surface coverage (θ) with concentration reflects enhanced occupation of active sites on the steel surface, leading to the formation of a protective barrier that restricts both anodic metal dissolution and cathodic hydrogen evolution reactions. The slight decline in efficiency at the highest concentrations suggests the establishment of an adsorption equilibrium in which surface saturation is reached and additional inhibitor molecules remain in the bulk solution without contributing significantly to further protection. This behaviour is characteristic of adsorption-controlled inhibition mechanisms and supports the subsequent thermodynamic and adsorption isotherm analyses.

Adsorption isotherms analysis

Adsorption isotherm analysis constitutes a fundamental approach for elucidating the interaction mechanism between inhibitor molecules and the carbon steel surface in aggressive media. The magnitude of the standard free energy of adsorption ($\Delta G°_{ads}$) provides important insight into the nature of the adsorption process. Values close to -20 kJ mol^{-1} or less negative are typically associated with electrostatic interactions between charged inhibitor species and the metal surface, characterizing a predominantly physical adsorption (physisorption) mechanism. In contrast, $\Delta G°_{ads}$ values around -40 kJ mol^{-1} or more negative indicate stronger interactions involving charge sharing or charge transfer between the inhibitor molecules and the metal surface, leading to the formation of coordinated covalent bonds and suggesting a chemisorption-controlled process [29].

The adsorption behaviour of the inhibitor molecules on the carbon steel surface was evaluated using the surface coverage values (θ) obtained from gravimetric measurements and the corresponding inhibitor concentrations (C). The experimental data were fitted to the Langmuir, Freundlich, Temkin, Flory-Huggins and Frumkin adsorption isotherms aiming to determine the model that best describes the metal-inhibitor interaction. The regression coefficients (R^2) and linearized equations obtained for each model are presented in Table 3.

Table 3. *Evaluation of adsorption isotherms parameters adjustments*

Adsorption isotherms	R^2	Line's equation
Langmuir (C/θ *vs.* C): $C/\theta = 1/K + C$	0.9981	$y = 0.9182x - 0.1311$
Freundlich ($\log\theta$ *vs.* $\log C$): $\theta = K_f C^{1/n}$	0.6907	$y = 7.4523x + 0.9989$
Temkin (θ *vs.* $\log C$): $\theta = (2.303/a)\log K + (2.303/a)\log C$	0.6948	$y = 3.9821x - 2.9259$
Flory-Huggins ($\log(\theta/C)$ *vs.* $\log(1-\theta)$): $\log(\theta/C) = \log K + x\log(1-\theta)$	0.8838	$y = 0.7317x - 0.5440$
Frumkin ($\log(\theta/(1-\theta)C)$ *vs.* θ): $\log(\theta/(1-\theta)C) = \log K + g\theta$	0.0900	$y = 0.1101x + 0.9009$

Adsorption isotherm parameters: K is the equilibrium adsorption constant; K_f is the Freundlich adsorption constant; n represents the adsorption intensity (indicating the favourability of the process); a and g correspond to the lateral interaction parameters between adsorbed species; and x denotes the number of water molecules replaced by each adsorbed inhibitor molecule [9,12]

A comparative analysis of the correlation coefficients clearly indicates that the Langmuir isotherm provides the best mathematical fit to the experimental data, with an exceptionally high regression coefficient (R^2 = 0.9981). This value is significantly higher than those obtained for the Flory-Huggins (R^2 = 0.8838), Temkin (R^2 = 0.6948), Freundlich (R^2 = 0.6907) and Frumkin (R^2 = 0.0900) models. The near-unity R^2 value for the Langmuir model strongly supports the conclusion that the adsorption process follows an ideal monolayer adsorption mechanism [9,12].

According to the Langmuir model, adsorption occurs at specific homogeneous active sites on the metal surface, with each site accommodating a single inhibitor molecule and without significant lateral interactions between adsorbed species [9]. The slope close to unity ($y = 0.9182x - 0.1311$) further reinforces the predominance of a monolayer adsorption mechanism, suggesting that surface coverage increases proportionally with inhibitor concentration until saturation of available active sites is reached.

Such adsorption is typically associated with electrostatic interactions between protonated organic species and the negatively charged metal surface [8], as well as donor-acceptor interactions involving heteroatoms (such as oxygen and nitrogen) and vacant iron orbitals [26]. This adsorption mechanism effectively blocks active sites, reducing the available area for anodic iron dissolution and cathodic hydrogen evolution reactions [9,12].

From the linearized Langmuir isotherm, the adsorption equilibrium constant (K_{ads}) can be obtained from the reciprocal of the intercept ($1/K$). Based on the fitted linear equation, the calculated adsorption equilibrium constant was 7.6278 L g^{-1}. The determination of K_{ads} enables the thermodynamic evaluation of the adsorption process through calculation of the standard Gibbs free energy of adsorption ($\Delta G°_{ads}$), according to Equation (4) [1], where T represents the absolute temperature (298 K in the present study), R is the universal gas constant (8.3147 J mol^{-1} K^{-1}), and C_{H_2O} is the molar concentration of water in the solution (55.5 mol L^{-1}).

$$\Delta G°_{ads} = -RT \ln(C_{H_2O} K_{ad}) \quad (4)$$

Using these parameters, the calculated value of $\Delta G°_{ads}$ was -14.986 kJ mol^{-1}. The negative value confirms that the adsorption process of the inhibitor molecules onto the carbon steel surface is thermodynamically spontaneous under the studied conditions. Furthermore, the magnitude of $\Delta G°_{ads}$ indicates that the adsorption process in this study can be classified predominantly as physical adsorption (physisorption), a weak interaction [9,12,29].

Electrochemical analysis

According to the results obtained from the gravimetric corrosion tests, the ethanolic extract of *Annona muricata* leaves exhibited a concentration-dependent inhibition behaviour. Although inhibition efficiency generally increased with extract concentration, the system containing 8 vol.% showed a slight decrease in corrosion inhibition performance compared with the lower concentrations.

As previously discussed, this behaviour may be associated with possible saturation of adsorption sites or changes in the adsorption-desorption equilibrium at higher inhibitor concentrations, which can affect the stability and compactness of the protective film formed on the metal surface. Therefore, to focus the electrochemical investigation on the concentration range that exhibited the most effective corrosion inhibition performance, the electrochemical measurements were carried out using extract concentrations up to 6 vol.%, as well as the uninhibited solution (negative control).

Open circuit potential

Initially, the evolution of the open circuit potential (OCP) was monitored to evaluate stabilization of the metal/electrolyte interface prior to the electrochemical measurements. The OCP for SAE 1008 carbon steel immersed in 1.0 mol L^{-1} HCl solution in the absence and presence of different concentrations (1, 2, 4 and 6 vol.%) of ethanolic extract of *Annona muricata* leaves was monitored for 3600 s (Figure 2).

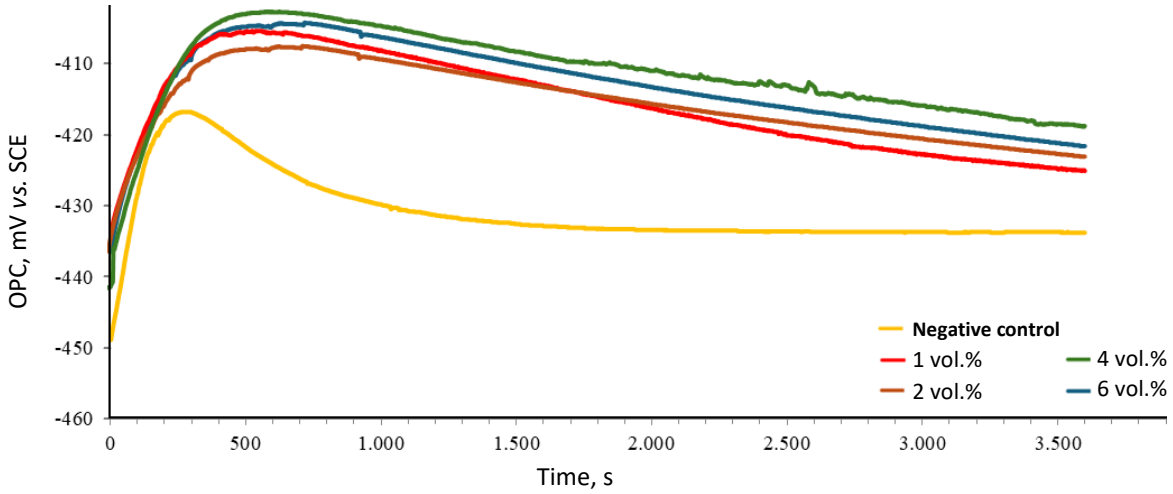

Figure 2. *Open circuit potential as a function of immersion time for SAE 1008 carbon steel in 1.0 mol L^{-1} HCl solution in the absence (negative control) and presence of different concentrations of Annona muricata leaf ethanolic extract*

In the uninhibited solution, the OCP rapidly shifts toward more negative values, indicating the active dissolution of steel in the aggressive acidic medium (Figure 2). In contrast, the addition of the plant extract results in a gradual displacement of the potential toward less negative values. This behaviour suggests the progressive adsorption of organic molecules present in the extract onto the steel surface, forming a protective layer that modifies the interfacial electrochemical processes during the initial immersion period.

Although the displacement in corrosion potential is relatively moderate, this tendency indicates that the inhibitor influences both anodic metal dissolution and cathodic hydrogen evolution reactions. Such behaviour is characteristic of mixed-type corrosion inhibitors, which reduce the overall corrosion rate by blocking active surface sites involved in both electrochemical reactions [30].

Electrochemical impedance spectroscopy

The electrochemical impedance spectroscopy (EIS) results obtained for SAE 1008 carbon steel in 1.0 mol L^{-1} HCl solution in the absence and presence of different concentrations (1, 2, 4 and 6 vol.%) of the ethanolic extract of *Annona muricata* leaves are presented in Figures 3a and Figure 3b as Nyquist and Bode diagrams respectively, while the equivalent electrical circuit (EEC) used to fit the experimental data is shown in Figure 3c. This equivalent circuit has been widely used in the literature to adequately describe EIS responses in systems containing different corrosion inhibitors [9,12,15,31].

The Nyquist diagrams exhibit a single depressed capacitive semicircle for all investigated systems, indicating that the corrosion process is mainly controlled by charge transfer at the metal/electrolyte interface [1,6,15]. After the addition of the ethanolic extract of *Annona muricata* leaves, a pronounced enlargement of the semicircle diameter is observed, demonstrating a significant increase in the corrosion resistance of the steel surface [32].

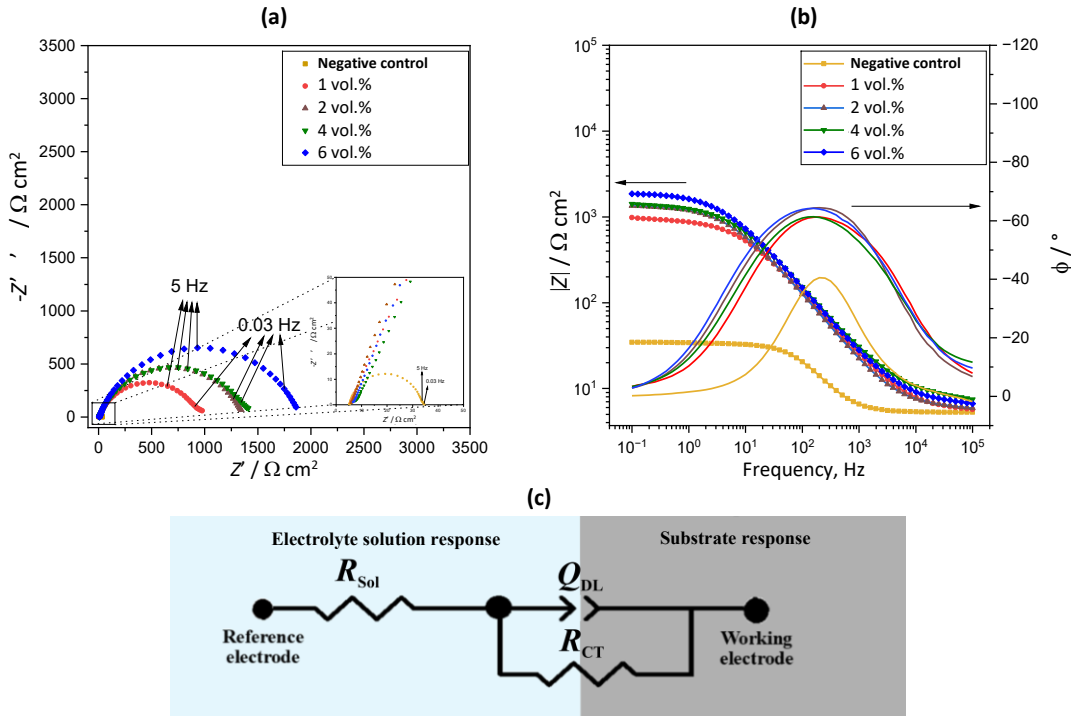

Figure 3. *(a) Nyquist and (b) Bode diagrams for SAE 1008 carbon steel immersed in 1.0 mol L^{-1} HCl solution in the absence and presence of different concentrations of ethanolic extract of* Annona muricata *leaves; (c) equivalent electrical circuit used to fit the experimental EIS data, where* R_{sol} *represents the solution resistance,* R_{CT} *the charge transfer resistance and* Q_{DL} *the capacitive parameter of the constant phase element associated with the electrical double layer*

After the addition of the ethanolic extract of *Annona muricata* leaves, a pronounced enlargement of the semicircle diameter is observed, demonstrating a significant increase in the corrosion resistance of the steel surface [32]. The depressed character of the semicircles indicates non-ideal capacitive behaviour, which is commonly attributed to surface heterogeneity, roughness [33,34], and the distribution of active corrosion sites on the steel surface [35].

The Bode diagrams (Figure 3b) further corroborate the electrochemical behaviour observed in the Nyquist diagrams. The progressive increase in the low-frequency impedance modulus ($|Z|$) with increasing extract concentration reflects an enhancement of the overall corrosion resistance resulting from the adsorption of phytochemical constituents on the steel surface. Moreover, the inhibited systems exhibit broader peaks and higher phase angles, indicating a more capacitive interfacial response and the formation of a more homogeneous protective film.

The corrosion parameters obtained from the fitting procedure are summarized in Table 4. In the absence of the inhibitor (negative control), the Nyquist diagram presents a small semicircle (Figure 3a) with a charge transfer resistance (R_{CT}) of 28.82 Ω cm^2, indicating a fast corrosion process in the acidic chloride medium. The inhibition efficiencies (η / %) also reported in Table 4 were calculated using Equation 4 [15], where R_{CT0} and R_{CTi} represent the charge transfer resistance value in the absence and presence of the inhibitor, respectively.

$$\eta = \frac{R_{CTi} - R_{CT0}}{R_{CT0}} 100 \quad (4)$$

The R_{CT} values increase drastically with increasing inhibitor concentration. This substantial increase in charge transfer resistance indicates that the adsorption of phytochemical constituents effectively hinders the electrochemical reactions occurring at the steel/electrolyte interface [15,35].

This protective adsorbed layer reduces the available active sites for charge transfer, thereby decreasing the corrosion rate and increasing the interfacial resistance.

Table 4. *Electrochemical parameters obtained from fitting the EIS data using the Randles equivalent circuit model for SAE 1008 carbon steel immersed in 1.0 mol L^{-1} HCl solution in the absence and presence of different concentrations) of ethanolic extract of* Annona muricata *leaves*

Concentration, vol.%	R_{Sol} / Ω cm²	R_{CT} / Ω cm²	Q_{DL} / μF cm^{-2} $s^{(\alpha-1)}$	α	η / %	θ
0 (negative control)	5.261	28.82	141.00	0.893	-	-
1	5.464	956.2	54.76	0.762	96.99	0.970
2	5.790	1355.0	50.12	0.787	97.87	0.979
4	7.422	1450.0	50.22	0.751	98.01	0.980
6	6.562	1891.0	45.46	0.773	98.48	0.985

Legend: α - CPE exponent describing surface heterogeneity.

Simultaneously, the reduction in the Q values of CPE suggests a decrease in the local dielectric constant and/or an increase in the thickness of the electrical double layer [33,34,36], which is commonly associated with the adsorption of organic molecules onto the metal surface. These findings are in line with the Langmuir adsorption behaviour obtained from the gravimetric measurements, indicating the formation of a compact organic monolayer.

At the same time, the solution resistance remains relatively constant, varying only slightly from 5.26 to 7.42 Ω cm^2. This behaviour suggests that the inhibitor does not significantly alter the conductivity of the electrolyte solution, and therefore the observed changes in impedance response are primarily associated with modifications occurring at the metal/electrolyte interface.

The interfacial capacitance behaviour was represented using a constant phase element (Q_{DL}), whose exponent (α) ranged between 0.751 and 0.893. The deviation of α from unity confirms the non-ideal capacitive behaviour of the system, which is typical for corroding metal surfaces [35,36]. The decrease in α values in the presence of the inhibitor suggests an increase in surface heterogeneity of the carbon steel surface [37].

In this sense, Q_{DL} are representative of non-ideal capacitive behaviour arising from surface heterogeneities such as roughness, porosity, and structural inhomogeneities [33]. These characteristics lead to dispersion in the impedance response over the frequency domain. The CPE parameter (Q) represents pseudo-capacitance and can be mathematically described by Equation (5) [37], which defines the impedance of the CPE. In this expression, $\omega = 2\pi f$ (f - frequency), and α is the dispersion exponent, with values ranging between 0 and 1. As α approaches unity, the CPE behaviour progressively converges to that of an ideal capacitor [34,35]. α value between 0.5 and 1.0 indicates the presence of interfacial heterogeneities and non-uniform current distribution across the electrode surface [35,36].

$$Z_{CPE} = \frac{1}{Q(j\omega)^{\alpha}} \quad (5)$$

The inhibition efficiency calculated from the R_{CT} increases significantly with increasing inhibitor concentration. These high efficiency values demonstrate the remarkable corrosion protection provided by the ethanolic extract of *Annona muricata* leaves.

As also previously discussed, this corrosion inhibition effect can be attributed to the adsorption of phytochemical constituents present in the extract, such as flavonoids, phenolic compounds, tannins, and alkaloids [2,16,24]. These organic molecules contain heteroatoms and π-electron systems that can interact with the metal surface through donor-acceptor interactions, forming an adsorbed

protective layer [24]. This film acts as a barrier that limits chloride-ion access and reduces the charge-transfer processes associated with the corrosion reaction [25,26].

Potentiodynamic polarization curves (Tafel slopes)

The potentiodynamic polarization curves for SAE 1008 carbon steel in 1.0 mol L^{-1} HCl solution in the absence and presence of different concentrations (1, 2, 4 and 6 vol.%) of ethanolic extract of *Annona muricata* leaves are presented in Figure 4, while the corresponding electrochemical kinetic parameters obtained from the Tafel slopes are summarized in Table 5. The inhibition efficiency (η) values also reported in Table 5 were calculated using Equation (6), where j_{Corr_0} and j_{Corr_i} represent the corrosion current density in the absence and presence of the inhibitor, respectively.

$$\eta = \frac{j_{Corr\_i} - j_{Corr\_0}}{j_{Corr\_0}} 100 \quad (6)$$

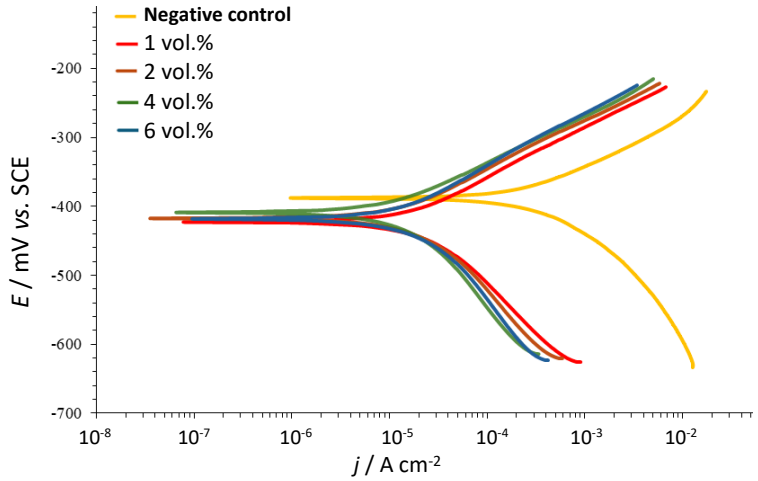

Figure 4. *Potentiodynamic polarization curves (PPC) after 120 min of immersion in 1.0 mol L^{-1} HCl solution in the absence and presence of different concentrations of ethanolic extract of Annona muricata leaves*

As shown in Figure 4, the addition of the plant extract significantly modifies both anodic and cathodic branches of the polarization curves when compared to the uninhibited system. The negative control exhibits a high corrosion current density, indicating an intense corrosion process in the acidic medium. In contrast, the inhibitor shifts the polarization curves toward lower current densities, demonstrating a substantial reduction in the corrosion rate of carbon steel.

Table 5. *Kinetics parameters obtained from potentiodynamic polarization curves (PPC) analyses after 1.0 mol L^{-1} HCl solution in the absence and presence of different concentrations of ethanolic extract of Annona muricata leaves*

C / vol.%	R_P / Ω cm²	E_{Corr} / mV *vs.* SCE	j_{Corr} / µA cm^{-2}	β_a / mV dec^{-1}	β_c / mV dec^{-1}	η / %	θ
0*	(35.7 ± 3.7)	(-388.0 ± 2.3)	(221.0 ± 1.1)	(67.5 ± 0.4)	(-78.6 ± 0.6)	-	-
1	(985.7 ± 5.5)	(-422.8 ± 1.7)	(16.5 ± 0.6)	(79.6 ± 0.6)	(-97.5 ± 0.7)	(92.53 ±1.10)	(0.925 ± 011)
2	(1454.0 ± 3.9)	(-417.9 ± 0.9)	(13.2 ± .4)	(80.5 ± 0.5)	(-93.2 ± 0.6)	(94.02 ± 0.78)	(0.940 ± 0.008)
4	(1481.0 ± 10.1)	(-417.8 ± 0.7)	(12.5 ± 0.8)	(84.4 ± 0.4)	(-89.7 ± 0.4)	(94.30 ± 0.82)	(0.943 ± 0.008)
6	(1853.0 ± 9.6)	(-408.0 ± 2.5)	(9.9 ± 0.7)	(70.7 ± 0.7)	(-100.0 ± 0.9)	(95.52 ± 1.27)	(0.955 ± 0.13)

*negative control; R_P - polarization resistance; E_{Corr} - corrosion potential; j_{Corr} - corrosion current density; β_a - anodic Beta coefficient; βc - cathodic Beta coefficient; η - inhibition efficiency calculated from j_{Corr} values;

This behaviour is confirmed by the corrosion current density (j_{Corr}) values obtained from the Tafel extrapolation. In the uninhibited solution, the j_{Corr} value is (221.0 ± 1.1) µA cm^{-2}, whereas in the presence of the ethanolic extract the current density decreases drastically. This pronounced

decrease indicates that the extract effectively suppresses the electrochemical reactions responsible for corrosion.

A progressive increase in polarization resistance (R_P) is also observed with increasing inhibitor concentration. This increase reflects enhanced resistance to charge transfer at the metal/electrolyte interface, consistent with the electrochemical impedance spectroscopy results and in line with the gravimetric observations.

The corrosion potential (E_{Corr}) values exhibit relatively small shifts in the presence of the inhibitor, varying from -388 ± 2.3 mV (inhibitor absence) to values between -422.8 ± 1.7 and -408.0 ± 2.5 mV when the extract is added. Since the displacement in E_{Corr} is less than 85 mV relative to the negative control solution, the inhibitor can be classified as a mixed-type corrosion inhibitor according to conventional electrochemical criteria [30,38]. This indicates that the ethanolic extract of *Annona muricata* leaves affects both anodic metal dissolution and cathodic hydrogen evolution reactions.

The inhibition efficiency calculated from the corrosion current density values increases with increasing inhibitor concentration. These high efficiency values confirm the protective effect of the ethanolic extract of *Annona muricata* leaves against carbon steel corrosion in acidic media, due to reasons previously discussed [24-26].

Although the inhibition efficiencies determined by gravimetric and electrochemical techniques differ slightly at the highest inhibitor concentration, this behaviour is not unusual because these techniques evaluate different aspects of the corrosion process. Weight-loss measurements represent the cumulative metal dissolution over the entire immersion period and therefore reflect the long-term protective performance of the inhibitor. In contrast, electrochemical impedance spectroscopy and potentiodynamic polarization curves are instantaneous techniques that evaluate the electrochemical condition of the metal/electrolyte interface at the time of measurement.

At higher extract concentrations, the adsorbed phytochemical layer may undergo molecular rearrangement or partial aggregation, slightly affecting its long-term protective stability while still providing a highly resistive interfacial film that effectively hinders charge transfer. Consequently, the electrochemical techniques may continue to indicate increasing interfacial protection, whereas the gravimetric method reflects the integrated corrosion behaviour during prolonged exposure.

Overall, the electrochemical evaluation results are in good agreement with the weight-loss measurements; all techniques indicate that 6 vol.% ethanolic extract of *Annona muricata* leaves acts as an efficient corrosion inhibitor for SAE 1008 carbon steel in 1.0 mol L^{-1} HCl solution.

Surface morphology and chemical characterization

Scanning electron microscopy analysis

The surface morphology of SAE 1008 carbon steel before and after immersion in 1 mol L^{-1} HCl solution, in the absence and presence of the ethanolic extract of *Annona muricata* leaves, was investigated by scanning electron microscopy (SEM), as presented in Figure 5. The micrograph of the polished steel surface prior to exposure to the corrosive medium (Figure 5a) shows a relatively smooth morphology characterized mainly by the parallel grinding lines produced during the mechanical polishing process. No evidence of corrosion products or localized attack is observed, indicating that the metallic surface remained intact before immersion.

In contrast, the sample immersed for 2 hours in the uninhibited 1.0 mol L^{-1} HCl solution (Figure 5b) exhibits a highly deteriorated surface morphology. The micrograph reveals the presence of irregular corrosion products and a rough, heterogeneous surface with pronounced degradation features.

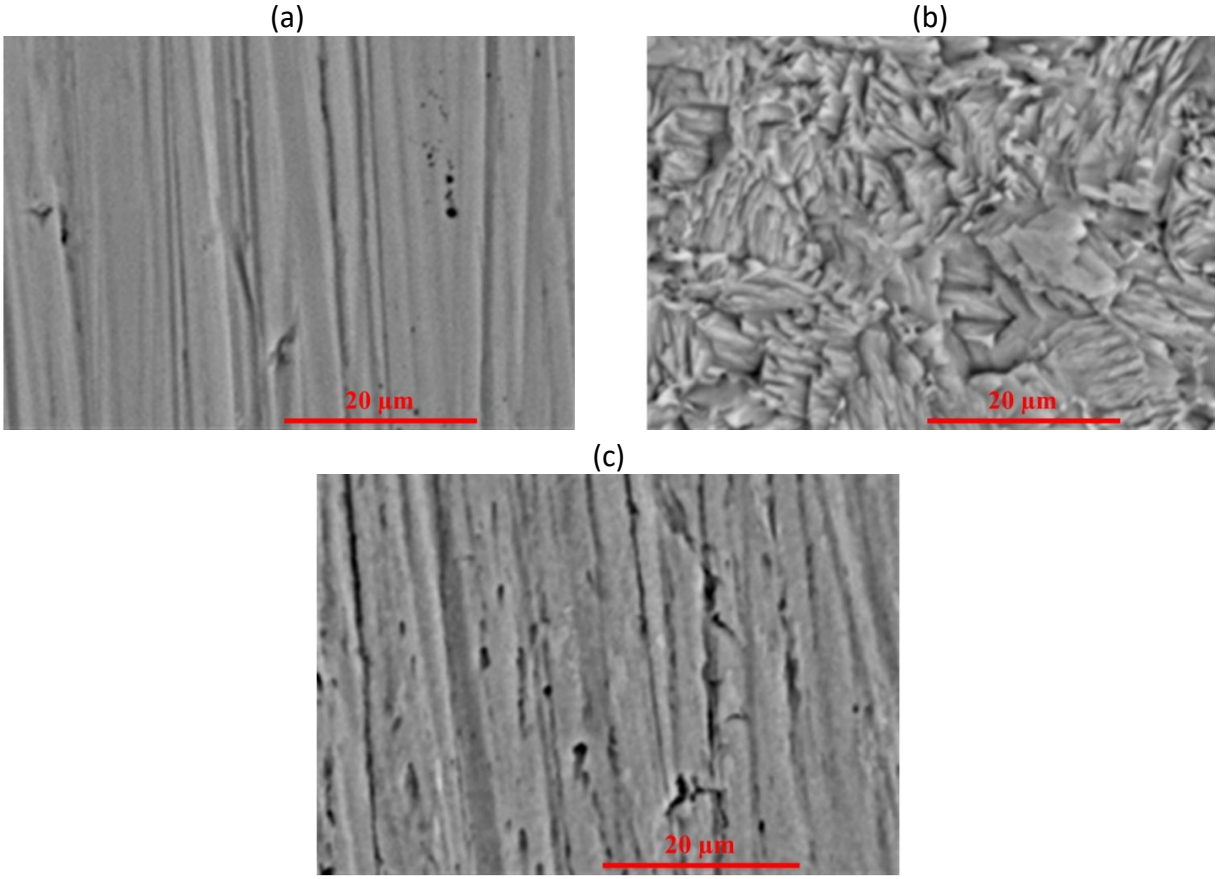

Figure 5. *Scanning electron microscopy (SEM) micrographs of SAE 1008 carbon steel surfaces: (a) polished steel surface before immersion; (b) steel surface after immersion (2 hours) in 1 mol L^{-1} HCl solution; (c) steel surface after immersion (2 hours) in 1.0 mol L^{-1} HCl solution containing 6 vol.% ethanolic extract of Annona muricata leaves*

The formation of these corrosion products is associated with the active dissolution of iron in the acidic medium, resulting in the development of corrosion layers and localized attack sites. The corrosion products formed under these conditions are poorly adherent and unstable, which facilitates their continuous detachment from the surface. Consequently, fresh metallic areas remain exposed to the aggressive environment, allowing the corrosion process to proceed continuously [39].

However, a significantly different morphology is observed when the steel surface is exposed to the corrosive solution containing 6 vol.% of the ethanolic extract of *Annona muricata* leaves (Figure 5c). In this case, the surface appears considerably smoother and more homogeneous compared to the uninhibited sample. The polishing grooves are still partially visible, suggesting that the aggressive action of the acid was strongly suppressed. This behaviour indicates the formation of a protective film on the metal surface, which acts as a barrier against the penetration of aggressive species from the electrolyte.

Similar surface protection behaviour has been reported for other plant-derived corrosion inhibitors. Comparable morphological improvements have also been described for castor bark powder [40], cocoa bean shell extract [1], *Pistia stratiotes* leaf extract [6], and malt bagasse extract [32], where the adsorption of phytochemical constituents leads to the formation of protective films that mitigate surface degradation in acidic media due to adsorption-driven inhibition mechanisms.

These observations align with electrochemical results from impedance spectroscopy and potentiodynamic polarization measurements, which showed a substantial increase in charge-transfer resistance and a decrease in corrosion current density in the presence of the inhibitor.

Raman spectroscopy analysis

Raman spectroscopy was employed to investigate the chemical interactions between the organic molecules present in the ethanolic extract of *Annona muricata* leaves and the steel surface after immersion in the acidic medium. The Raman spectra obtained for the solid inhibitor extract, the steel surface exposed to the inhibited solution, and the steel surface exposed to the uninhibited solution are presented in Figure 6 and corresponding chemical groups are summarized in Table 06.

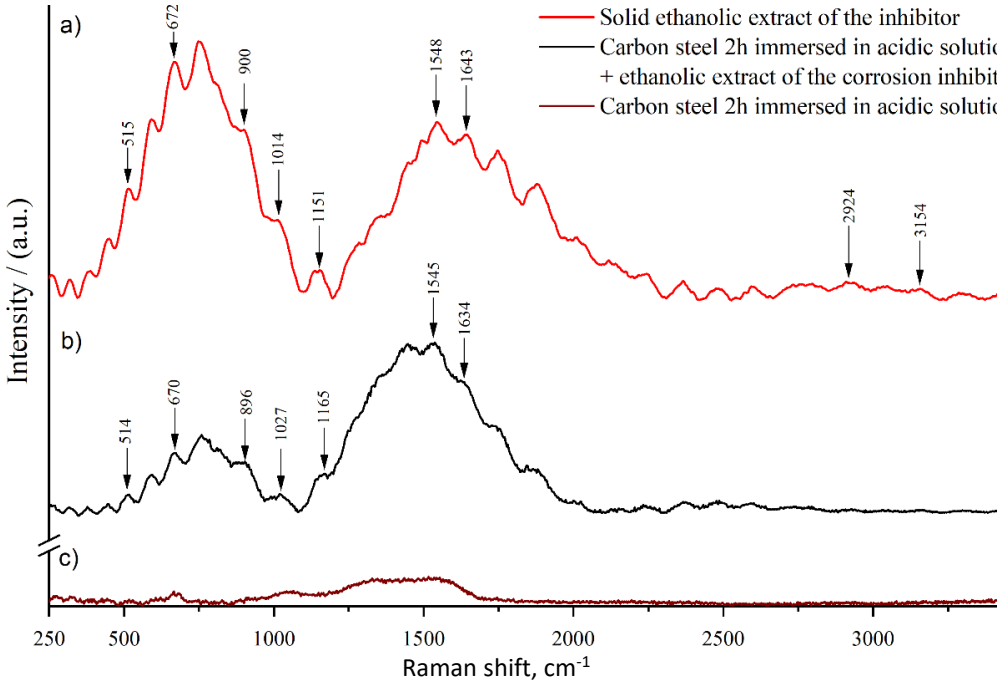

Figure 6. *Raman spectra of: (a) solid ethanolic extract of Annona muricata leaves; (b) steel surface after 2 h immersion in 1.0 mol L^{-1} HCl solution containing 6 vol.% inhibitor extract; (c) steel surface after 2 h immersion in 1.0 mol L^{-1} HCl solution without inhibitor*

Table 6. *Raman band identification for the ethanolic extract of Annona muricata leaves and for the carbon steel surface immersed in the absence and the presence of the corrosion inhibitor*

Raman shift, cm^{-1}	Corresponding group	Reference
~515	In-plane bending vibrational modes of aromatic rings.	[41]
~670	Out-of-plane vibrational modes of aromatic rings.	[41-43]
~900	Out-of-plane C-H deformation in benzene.	[41]
~1030	In-plane vibrational modes of aromatic rings.	[41,42]
~1165	In-plane C-H deformation	[41,44]
~1545	Aromatic C=C stretching vibrations and weak CH_2 vibrational modes	[41-44]
~1645	C=N and C=O stretching vibrations.	[41,43]
~2930	Asymmetric C-H stretching vibrations	[41,44]
~3155	N-H vibrational modes	[41,45]

Additional bands located at approximately 1150 cm^{-1} are related to C-H deformation modes within the aromatic structure [41,44]. The intense band observed around 1548 cm^{-1} can be assigned to C=C stretching vibrations of aromatic rings and to weak CH_2 vibrational modes [41,42,44]. Furthermore, the band near 1643 cm^{-1} is attributed to C=N and C=O stretching vibrations [41,43], indicating the presence of heteroatom-containing functional groups capable of interacting with the metallic surface.

The band at 2920 and 2930 cm^{-1} can be attributed to asymmetric C-H stretching vibrations, associated with aliphatic CH_2 and CH_3 groups present in the organic constituents of the ethanolic

extract [41,44]. A second band around 3155 cm^{-1} corresponds to N-H vibrational modes, indicating the presence of nitrogen-containing functional groups [41,45].

In the Raman spectrum obtained from the steel surface after immersion in the inhibited solution (Figure 6b), many bands appear at positions very close to those observed in the spectrum of the solid ethanolic extract. The presence of these bands indicates that organic molecules from the inhibitor extract remain adsorbed on the metal surface after immersion.

The preservation of these vibrational features suggests that the functional groups present in the extract interact with the steel surface through adsorption processes. Functional groups containing heteroatoms such as nitrogen and oxygen, as well as aromatic π-electron systems, can donate electron density to vacant orbitals of iron atoms, promoting the formation of an adsorbed protective layer [5,11,40].

On the other hand, the Raman spectrum of the steel surface exposed to the uninhibited acidic solution (Figure 6c) shows a very weak signal with the absence of the characteristic organic bands observed in the inhibited system, as expected. This result confirms that no organic protective film is present on the surface in the absence of the inhibitor.

Conclusions

The present study demonstrated that the ethanolic extract obtained from *Annona muricata* leaves acts as an effective green corrosion inhibitor for SAE 1008 carbon steel in acidic medium. Gravimetric measurements revealed a significant reduction in corrosion rate in the presence of the extract, confirming its protective effect and indicating that the inhibition efficiency increases with inhibitor concentration up to an optimum value (6 vol.%).

Adsorption studies showed that the inhibition process is governed by the adsorption of organic molecules onto the steel surface, forming a protective barrier that limits the interaction between the metal and the aggressive electrolyte with better fitting of Langmuir isotherm (R^2 = 0.9981). The calculated Gibbs free energy of adsorption presented negative values ($\Delta G°_{ads}$ = −14.986 kJ mol^{-1}), confirming that the adsorption process occurs spontaneously and is predominantly associated with physical monolayer adsorption mechanisms.

Electrochemical analyses further confirmed the inhibitory action of the extract. Electrochemical impedance spectroscopy revealed a marked increase in charge transfer resistance in the presence of the inhibitor, which suggests the formation of a protective interfacial layer that restricts corrosion reactions. Potentiodynamic polarization curves showed a significant decrease in corrosion current density, demonstrating that the extract acts as a mixed-type inhibitor by simultaneously reducing both anodic metal dissolution and cathodic hydrogen evolution reactions with high efficiency (η = 95.52 %) at 6 vol.% ethanolic extract of *Annona muricata* leaves.

Surface characterization techniques supported the electrochemical findings. Scanning electron microscopy showed severe surface damage in the uninhibited solution, whereas the samples exposed to the inhibited medium exhibited a considerably smoother surface morphology. Raman spectroscopy confirmed the presence of organic species from the extract adsorbed on the steel surface, with characteristic vibrational bands associated with functional groups such as aromatic rings, C=C, C=N, C=O, and N-H.

The results demonstrate that the ethanolic extract of *Annona muricata* leaves represents a promising environmentally friendly corrosion inhibitor for carbon steel in acidic environments, offering potential applications in industry.

Acknowledgements: *The authors would like to thank the Corrosion Laboratory of Chemical Engineering and the Textile Faculty of UNI for the support provided in the electrochemical tests and the characterization tests. The authors are grateful to the Vice-Rectorate for Research of the Universidad Nacional de Ingeniería. This study was financed in part by the Coordenação de Aperfeiçoamento de Pessoal de Nível Superior - Brazil (CAPES) - Financial Code 001, for a research grant to Gabriel A. Carrijo-Gonçalves (grant number: 88887.680349/2022-00).*

References

[1] M. C. F. de Carvalho, N. M. S. de Almeida, I. M. F. C. R. e Silva, F. Cotting, I. V. Aoki, V. R. Capelossi, Electrochemical and Economic Evaluation of the Cocoa Bean Shell as a Corrosion Inhibitor in Acidic Medium, *Materials Research* **25** (2022) e20210125. https://doi.org/10.1590/1980-5373-mr-2021-0125

[2] N. Kumar, P. Anunay, S. Kumar, L. K. Meena, D. Singh, An overview on emerging green organic corrosion inhibitors: sustainable solution for oil and gas industrial applications, *RSC Advances* **16** (2026) 3909-3948. https://doi.org/10.1039/D5RA08166A

[3] B. Mangla, G. Ji, Kajal, K. Rawat, H. Kaushik, K. Mittal, P. Vashishth, H. Bairagi, D.K. Sharma, H. Kumar, R. Sehrawat, Synthesis of ethanol extract of rose petal and its coating on mild steel for corrosion prevention in sodium chloride solutions, *Next Materials* **12** (2026) 102007. https://doi.org/10.1016/j.nxmate.2026.102007

[4] B. Mangla, G. Ji, K. Kajal, K. Rawat, H. Kaushik, K. Mittal, R. Sehrawat, P. Vashishth, H. Bairagi, D.K. Sharma, H. Kumar, Comprehensive study of garlic peel extract coating against mild steel corrosion in saline medium, *Discover Chemical Engineering* **6** (2026) 13 https://doi.org/10.1007/s43938-026-00110-6

[5] T. Prošek, P. Keil, K. Popova, Corrosion Protection and Sustainability: Why Are the Two Concepts Inherently Intertwined, *Corrosion and Materials Degradation* **6** (2025) 38. https://doi.org/10.3390/cmd6030038

[6] A. Carmona-Hernandez, M. C. Barreda-Serrano, H. A. Saldarriaga-Noreña, R. López-Sesenes, J. G. González-Rodríguez, E. Mejía-Sánchez, J. A. Ramírez-Cano, R. Orozco-Cruz, R. Galván-Martínez, Insight into the Corrosion Inhibition Performance of Pistia stratiotes Leaf Extract as a Novel Eco-Friendly Corrosion Inhibitor for Mild Steel in 1 M HCl Solution, *Molecules* **29** (2024) 5243. https://doi.org/10.3390/molecules29225243

[7] R. M. Bandeira, F. P. Lima, M. S. Nunes, E. C. dos Santos, J. R. dos Santos Júnior, J. M. E. de Matos, C. M. Feitosa, M. Rai, S. Bhattarai, D. Das Mulmi, The green plant-based corrosion inhibitors—a sustainable strategy for corrosion protection, *Surface Science and Technology* **3** (2025) 19. https://doi.org/10.1007/s44251-025-00084-7

[8] M. Abdallah, H. M. Altass, B. A. AL Jahdaly, M. M. Salem, Some natural aqueous extracts of plants as green inhibitor for carbon steel corrosion in 0.5 M sulfuric acid, *Green Chemistry Letters and Reviews* **11** (2018) 189-196. https://doi.org/10.1080/17518253.2018.1458161

[9] M. Abdallah, M. Alfakeer, F. H. Al-abdali, M. Sobhi, H. Hawsawi, D. F. Seyam, S. S. Al-Juaid, R. S. Abdel Hameed, Insights into the effectiveness of natural Mentha oil in mitigating the corrosion of carbon steel in sulfuric acid, *Green Chemistry Letters and Reviews* **18** (2025) 2527724. https://doi.org/10.1080/17518253.2025.2527724

[10] A. A. Al-Amiery, W. N. R. W. Isahak, W. K. Al-Azzawi, Corrosion Inhibitors: Natural and Synthetic Organic Inhibitors, *Lubricants* **11** (2023) 174. https://doi.org/10.3390/lubricants11040174

[11] L. S. Barreto, A. M. Santos, T. F. de Almeida, D. R. Silva, F. Cotting, V. R. Capelossi, Application of a Mix of Vegetables Residues as Inhibitor for Carbon Steel, *Materials Research* **25** (2022) e20200440. https://doi.org/10.1590/1980-5373-mr-2020-0440

[12] M. Abdallah, K. A. Soliman, M. Alfakeer, A. M. Al-bonayan, M. T. Alotaibi, H. Hawsawi, O. A. Hazazi, R. S. Abdel Hameed, M. Sobhi, Mitigation effect of natural lettuce oil on the corrosion of mild steel in sulfuric acid solution: chemical, electrochemical, computational aspects, *Green Chemistry Letters and Reviews* **16** (2023) 2249019. https://doi.org/10.1080/17518253.2023.2249019

[13] S. Toprak Döşlü, L. ERCAN, Corrosion Inhibition Mechanism and Stability of Quinic Acid as a Green Corrosion Inhibitor on Mild Steel, *ChemistryOpen* **15** (2026) e202500322. https://doi.org/10.1002/open.202500322

[14] B. Ergel, R. Yıldız, S. Arslanhan, M. F. Baran, A new green corrosion inhibitor for mild steel in 1 M HCl using *Erodium cicutarium* (L.) leaf extract: Insights from both theoretical and experimental methods, *Applied Surface Science* **722** (2026) 165587 https://doi.org/10.1016/j.apsusc.2025.165587

[15] A. Kumar, C. Das, *Duranta erecta* Fruit and Leaf Extracts as Green Corrosion Inhibitors for Mild Steel Protection in Hydrochloric Acid, *ACS Applied Engineering Materials* **4** (2026) 1113-1125. https://doi.org/10.1021/acsaenm.5c01138

[16] L. S. Barreto, G. A. C. Gonçalves, F. Cotting, V. R. Capelossi, *Agro-Industrial Residues and Plant Biomass as Green Corrosion Inhibitors*, in: *Encyclopedia of Green Materials*, Springer Nature Singapore, Singapore, 2022, 1-9. https://doi.org/10.1007/978-981-16-4921-9_177-1

[17] S. E. Hernández-Sánchez, J. P. Flores-De los Rios, H. A. Monreal-Romero, N. R. Flores-Holguin, L. M. Rodríguez-Valdez, M. Sánchez-Carrillo, A. D. Delgado, J. G. Chacón-Nava, Ruta graveolens Plant Extract as a Green Corrosion Inhibitor for 304 SS in 1 M HCl: Experimental and Theoretical Studies, *Metals* **14** (2024) 1267. https://doi.org/10.3390/met14111267

[18] C. Párraga, F. Rincón-Acosta, R. Barre-Zambrano, J. Vera-Cedeño, P. Vargas, F. Mendoza, Bioactive compounds and antioxidant activity of *Annona muricata* L. fruits located in Manabí, Ecuador, *Revista de La Facultad de Agronomía, Universidad Del Zulia* **41** (2024) e244107. https://doi.org/10.47280/RevFacAgron.v41.n1.07

[19] P. Srivastava, M. Singh, G. Devi, R. Chaturvedi, *Herbal Medicine and Biotechnology for the Benefit of Human Health*, in: *Animal Biotechnology,* A.S. Verma, A. Singh, Eds., Elsevier, 2014, pp. 563-575. https://doi.org/10.1016/B978-0-12-416002-6.00030-4

[20] N. S. Al-Radadi, Synthesis, Characterization, Antimalarial, Antimicrobial, and antioxidant activities of GNPs with Annona muricata leaf extract, *Arabian Journal of Chemistry* **18** (2025) 106081. https://doi.org/10.1016/j.arabjc.2024.106081

[21] J. I. Emmanuel, F. O. Ngasoh, A. Bello, V. C. Anye, B. Y. R. Surnam, A. P. Onwualu, Synergistic corrosion inhibition of phytochemicals on API 5L X65 steel in acidic media: an integrated experimental and computational approach, *Anti-Corrosion Methods and Materials* (2025) 1-22. https://doi.org/10.1108/ACMM-06-2025-3290

[22] A. V. Coria-Téllez, E. Montalvo-Gónzalez, E. M. Yahia, E. N. Obledo-Vázquez, Annona muricata: A comprehensive review on its traditional medicinal uses, phytochemicals, pharmacological activities, mechanisms of action and toxicity, *Arabian Journal of Chemistry* **11** (2018) 662-691. https://doi.org/10.1016/j.arabjc.2016.01.004

[23] S. Moghadamtousi, M. Fadaeinasab, S. Nikzad, G. Mohan, H. Ali, H. Kadir, *Annona muricata* (Annonaceae): A Review of Its Traditional Uses, Isolated Acetogenins and Biological Activities, *International Journal of Molecular Sciences* **16** (2015) 15625-15658. https://doi.org/10.3390/ijms160715625

[24] M. Kemel, Eco-friendly corrosion inhibition of steel using phenolic compounds from Cynara syriaca, *Journal of Industrial and Engineering Chemistry* **140** (2024) 617-630. https://doi.org/10.1016/j.jiec.2024.08.038

[25] D.-I. (Gheorghe) Răuță, E. Matei, S.-M. Avramescu, Recent Development of Corrosion Inhibitors: Types, Mechanisms, Electrochemical Behavior, Efficiency, and Environmental Impact, *Technologies* **13** (2025) 103. https://doi.org/10.3390/technologies13030103
[26] M. A. Ahmed, S. Amin, A. A. Mohamed, Current and emerging trends of inorganic, organic and eco-friendly corrosion inhibitors, *RSC Advances* **14** (2024) 31877-31920. https://doi.org/10.1039/D4RA05662K
[27] L. Patel, V. Sahu, R. Rawat, B. Jain, *Ionic liquids as green corrosion inhibitor*, in*: Computational Modelling and Simulations for Designing of Corrosion Inhibitors*, Elsevier, 2023, pp. 481-507. https://doi.org/10.1016/B978-0-323-95161-6.00014-X
[28] Y. L. Kobzar, K. Fatyeyeva, Ionic liquids as green and sustainable steel corrosion inhibitors: Recent developments, *Chemical Engineering Journal* **425** (2021) 131480. https://doi.org/10.1016/j.cej.2021.131480
[29] R. S. Abdel Hameed, Gh. M. S. Aleid, D. Mohammad, M. M. Badr, B. Huwaimel, M. Sh. Suliman, F. Alshammary, M. Abdallah, Spinacia oleracea Extract as Green Corrosion Inhibitor for Carbon Steel in Hydrochloric Acid Solution, *International Journal of Electrochemical Science* **17** (2022) 221017. https://doi.org/10.20964/2022.10.31
[30] H. Mobtaker, M. Azadi, N. Hassani, M. Neek-Amal, M. Rassouli, M. A. Bidi, The inhibition performance of quinoa seed on corrosion behavior of carbon steel in the HCl solution; theoretical and experimental evaluations, *Journal of Molecular Liquids* **335** (2021) 116183. https://doi.org/10.1016/j.molliq.2021.116183
[31] A. F. Shoair, M. M. A. H. Shanab, M. H. H. Mahmoud, Z. I. Zaki, H. M. Abdel-Ghafar, M. M. Motawea, Investigation on Effects of Avocado Extract as Eco-friendly Inhibitor for 201 Stainless Steel corrosion in Acidic Environment, *International Journal of Electrochemical Science* **17** (2022) 220642. https://doi.org/10.20964/2022.06.31
[32] T. F. de Almeida, M. C. F. de Carvalho, M. E. S. de Jesus, C. C. N. Kunrath, L. S. Barreto, F. D. R. Amado, V. R. Capelossi, Evaluation of the anticorrosion performance of malt bagasse as corrosion inhibitor for AISI 1020 carbon steel in acidic solution, *Revista Matéria (Rio de Janeiro)* **27** (2022) e13189. https://doi.org/10.1590/s1517-707620220002.1389
[33] R. de Levie, On the impedance of electrodes with rough interfaces, *Journal of Electroanalytical Chemistry and Interfacial Electrochemistry* **261** (1989) 1-9. https://doi.org/10.1016/0022-0728(89)87121-9
[34] R. De Levie, On impedance measurements: The determination of the double layer capacitance in the presence of an electrode reaction, *Electrochimica Acta* **10** (1965) 395-402. https://doi.org/10.1016/0013-4686(65)80055-X
[35] G. A. Carrijo-Gonçalves, B. P. da Silva, T. C. Veloso, V.R . Capelossi, Electrochemical and surface morphology characterizations of zinc electroplated coatings, *Surface Engineering* **41** (2025) 227-240. https://doi.org/10.1177/02670844251314127
[36] S. Holm, T. Holm, Ø. G. Martinsen, Simple circuit equivalents for the constant phase element, *PLoS One* **16** (2021) e0248786. https://doi.org/10.1371/journal.pone.0248786
[37] P. Zoltowski, On the electrical capacitance of interfaces exhibiting constant phase element behaviour, *Journal of Electroanalytical Chemistry* **443** (1998) 149-154. https://doi.org/10.1016/S0022-0728(97)00490-7
[38] G. Salinas-Solano, J. Porcayo-Calderon, L. M. Martinez de la Escalera, J. Canto, M. Casales-Diaz, O. Sotelo-Mazon, J. Henao, L. Martinez-Gomez, Development and evaluation of a green corrosion inhibitor based on rice bran oil obtained from agro-industrial waste, *Industrial Crops and Products* **119** (2018) 111-124. https://doi.org/10.1016/j.indcrop.2018.04.009
[39] M. Jia, P. Hu, G. Hu, Corrosion Layers on Archaeological Cast Iron from Nanhai I, *Materials* **15** (2022) 4980. https://doi.org/10.3390/ma15144980

[40] A. de M. Santos, T. F. De Almeida, F. Cotting, I. V. Aoki, H. G. de Melo, V. R. Capelossi, Evaluation of Castor Bark Powder as a Corrosion Inhibitor for Carbon Steel in Acidic Media, *Materials Research* **20** (2017) 492-505. https://doi.org/10.1590/1980-5373-mr-2016-0963

[41] A. Lecante, F. Robert, M. Lebrini, C. Roos, Inhibitive Effect of Siparuna Guianensis Extracts on the Corrosion of Low Carbon Steel in Acidic Media, *International Journal of Electrochemical Science* **6** (2011) 5249-5264. https://doi.org/10.1016/S1452-3981(23)18403-3

[42] L. Fengting, L. Suiqing, L. Xuefei, Study of PH Dependence of 2-Mercaptobenzothiazole by Surface Enhanced FT-Raman Scattering, *Spectroscopy Letters* **33** (2000) 901-907. https://doi.org/10.1080/00387010009350166

[43] D. R. Pompeu, Y. Larondelle, H. Rogez, O. Abbas, J. A. F. Pierna, V. Baeten, Characterization and discrimination of phenolic compounds using Fourier transform Raman spectroscopy and chemometric tools, *BASE* **22(1)** (2018) 13-28. https://doi.org/10.25518/1780-4507.16270

[44] T. Frosch, M. Schmitt, K. Schenzel, J. H. Faber, G. Bringmann, W. Kiefer, J. Popp, *In vivo* localization and identification of the antiplasmodial alkaloid dioncophylline A in the tropical liana *Triphyophyllum peltatum* by a combination of fluorescence, near infrared Fourier transform Raman microscopy, and density functional theory calculations, *Biopolymers* **82** (2006) 295-300. https://doi.org/10.1002/bip.20459

[45] S. Gunasekaran, G. Sankari, S. Ponnusamy, Vibrational spectral investigation on xanthine and its derivatives—theophylline, caffeine and theobromine, *Spectrochimica Acta A* **61** (2005) 117-127. https://doi.org/10.1016/j.saa.2004.03.030